Joint Research Centre

Comprehensive characterization of RAMSES hyper-spectral radiometers

Prepared by G. Zibordi,
European Commission, JRC, Ispra

The Fiducial Reference Measurement Network for Satellite Ocean Colour
4-5 October 2018 in NPL, Teddington, London, UK

Joint Research Centre

A measurement of any kind is incomplete unless accompanied with an estimate of the uncertainty associated with that measurement.

J. M. Palmer and B. G. Grant (2009). **The Art of Radiometry.** Bellingham: SPIE, 2009

Joint Research Centre

Calibration Equation

The conversion from relative to physical units of the radiometric quantity $\Im(\lambda)$ (either $E(\lambda)$ or $L(\lambda)$) at wavelength λ is performed through

$$\Im(\lambda) = C_{\Im}(\lambda)\, I_f(\lambda)\, \aleph(\lambda)\, DN(\Im(\lambda))$$

where $DN(\Im(\lambda))$ indicates the digital output corrected for the dark value, $C_{\Im}(\lambda)$ is the in–air absolute calibration coefficient (i.e., the absolute responsivity), $I_f(\lambda)$ is the immersion factor accounting for the change in responsivity of the sensor when immersed in water with respect to air, and $\aleph(\lambda)$ corrects for any deviation from the ideal performance of the measuring system.

In the case of an ideal radiometer $\aleph(\lambda)=1$, but in general

$$\aleph(\lambda)= \aleph_i(i(\lambda))\, \aleph_j(j(\lambda))\, \ldots \aleph_k(k(\lambda))$$

where $\aleph_i(i(\lambda))$, $\aleph_j(j(\lambda))$, …, and $\aleph_k(k(\lambda))$ are correction terms for different factors affecting the non-ideal performance of the considered radiometer (e.g., non-linearity, temperature response, polarization sensitivity, stray-light perturbations, spectral response, geometrical response, …).

Joint Research Centre

RAMSES dual-field of view above-water system

System for the simultaneous determination of L_w with 3 and 7 degrees full-angle field of view

RAMSES (TriOS) radiometers

- RAMSES-ACC irradiance sensors rely on a cosine collector of 3.5 mm radius, while RAMSES-ARC radiance sensors have a condenser lens defining a full-angle field-of-view of ~7 degrees.
- The foreoptics is coupled to a fiber bundle that feeds a ZEISS (Oberkochen, Germany) Monolithic Miniature Spectrometer (MMS-1) built on the Hamamatsu (Ichino-cho, Japan) S3904 256-channel NMOS array.
- The integration time can be set between 4 ms and 8192 ms.
- The spectral resolution is approximately 10 nm with average spectral sampling of 3.3 nm in the 320 nm–950 nm interval.

Immersion Factor I_f (radiance)

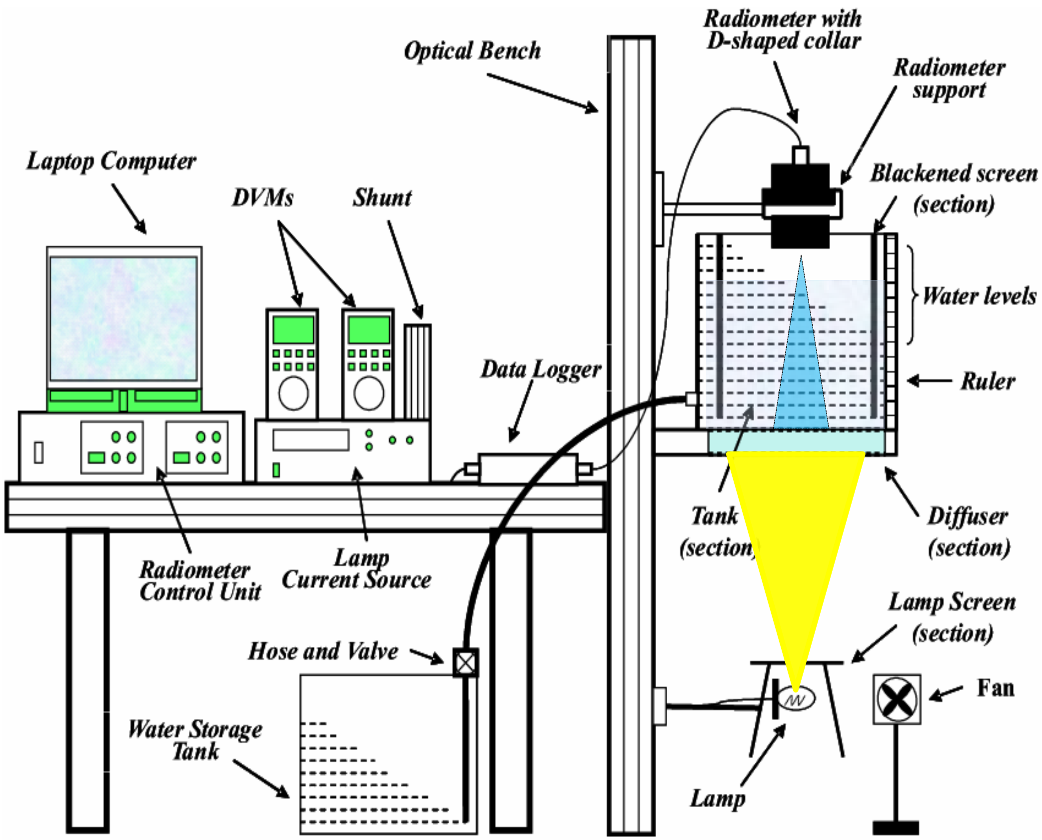

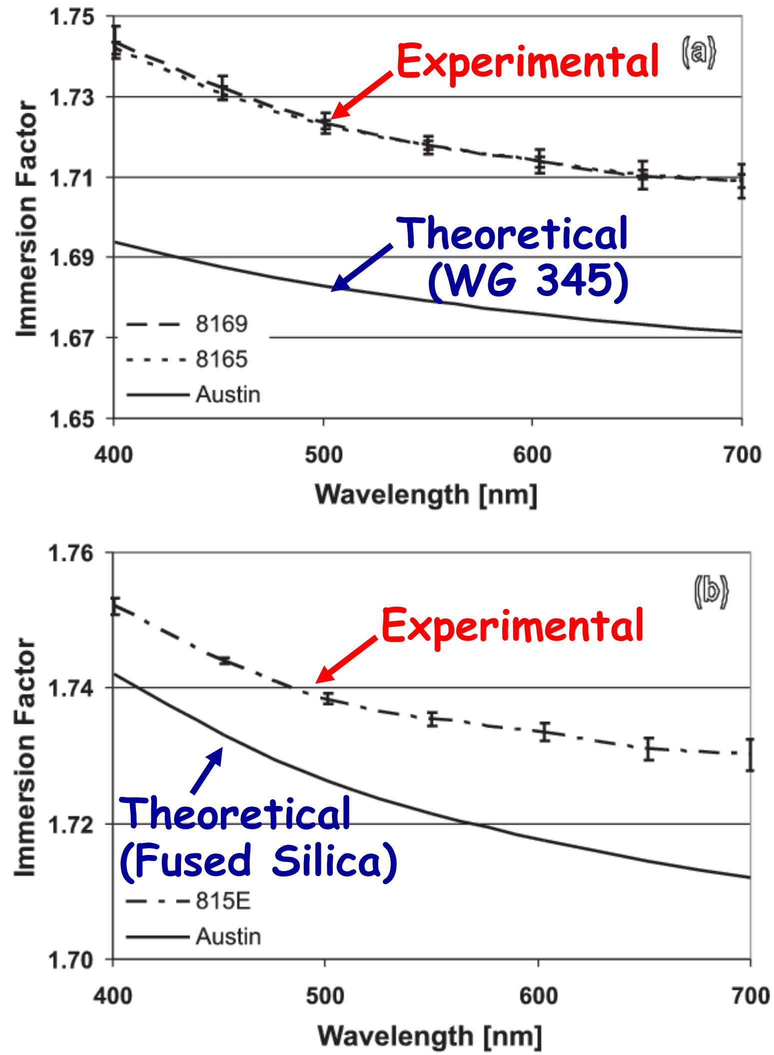

G.Zibordi. Immersion factor of in-water radiance sensors: assessment for a class of radiometers. *Journal of Atmospheric and Oceanic Technology*, 2006.

Immersion Factor I_f (irradiance)

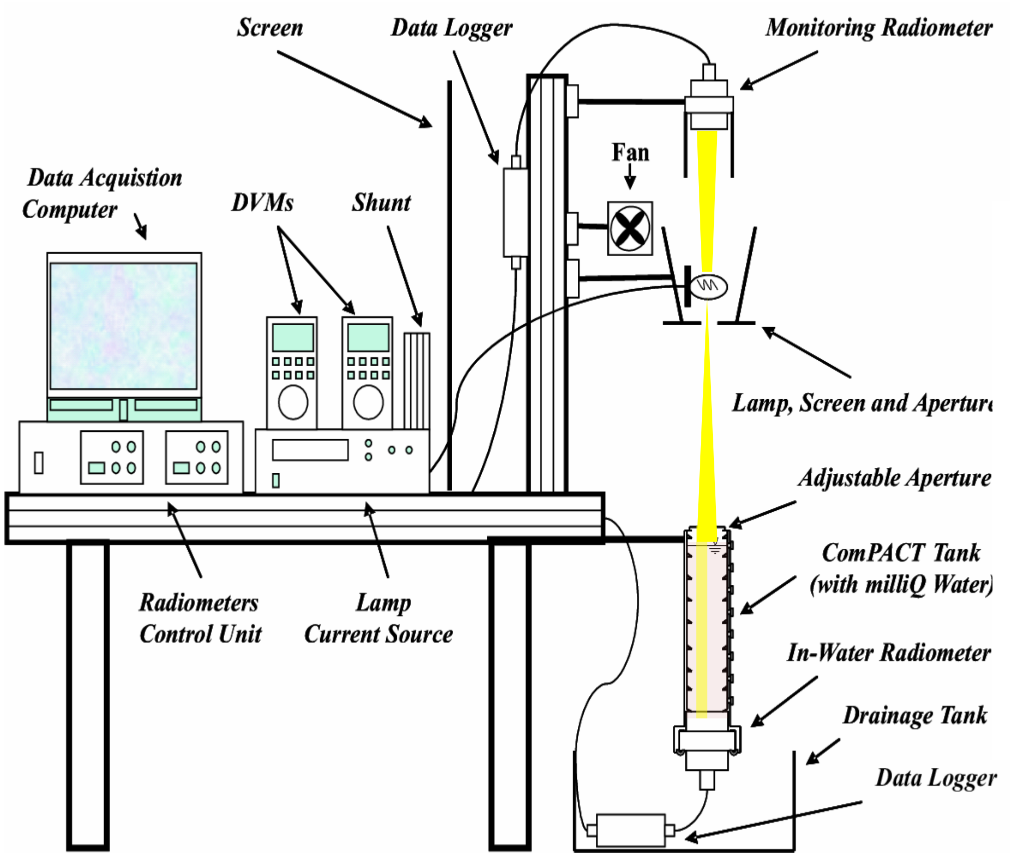

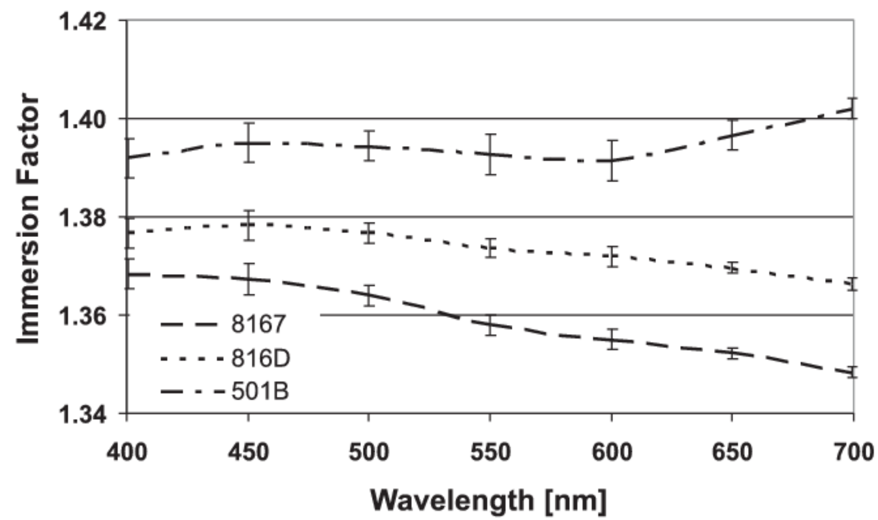

G.Zibordi et al. Characterization of the immersion factor for a series of in–water optical radiometers. Journal of Atmospheric and Oceanic Technology, 21:501-514, 2004.

Cosine Error for Irradiance Sensors

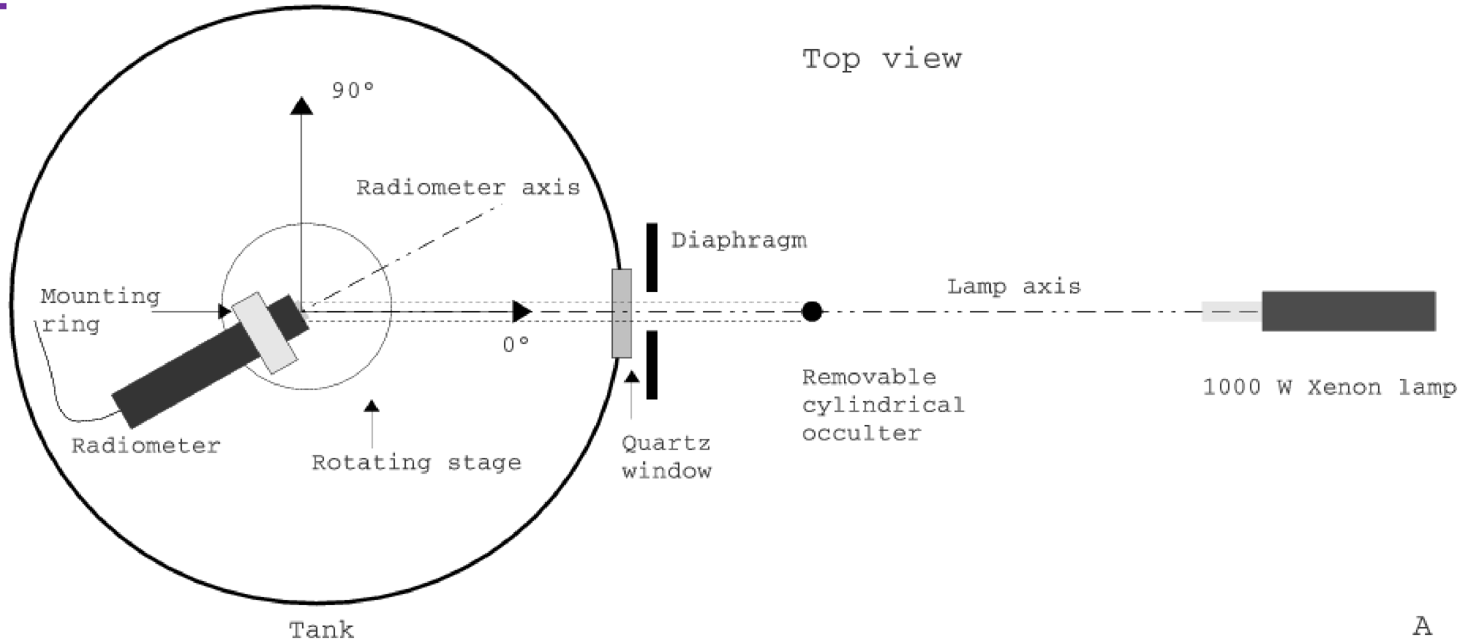

Schematic of the JRC ARCS system including lamp, water-tank and rotary stage

S. Mekaoui and G. Zibordi. Cosine error for a class of hyperspectral irradiance sensors, Metrologia 50 (2013).

B

Joint Research Centre

In-air and in-water spectral results

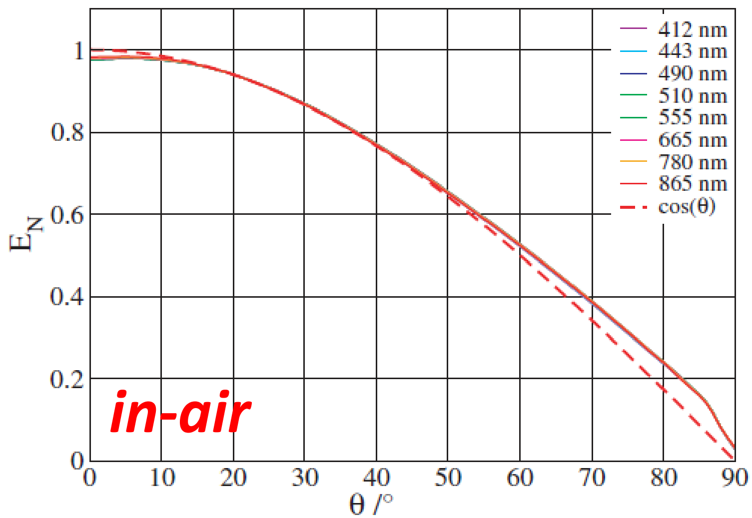

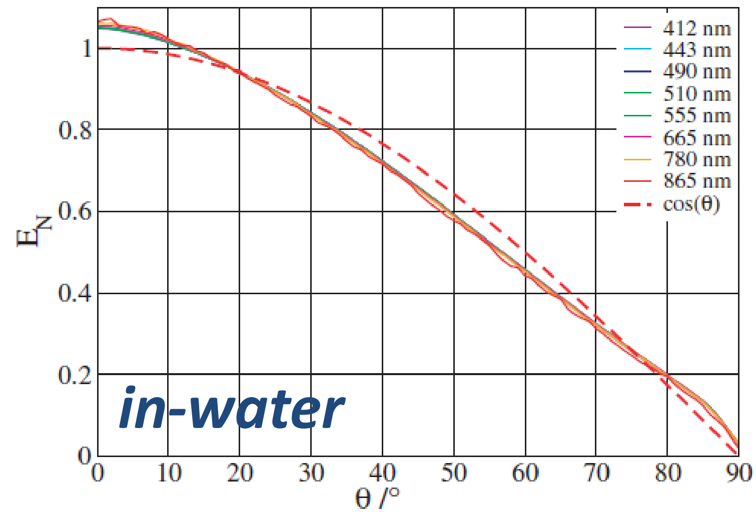

Angular response normalized at 20⁰

$$E_N(\phi, \theta, \lambda) = [E(\phi, \theta, \lambda)\cos(20)]/E_0(\phi, 20, \lambda)$$

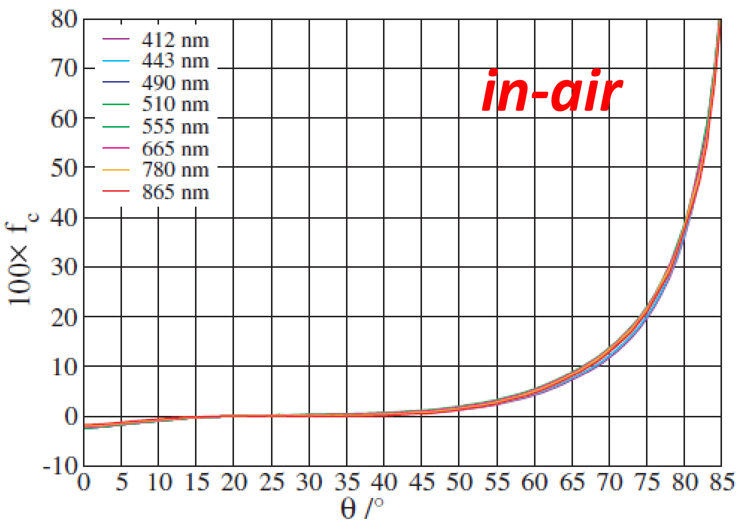

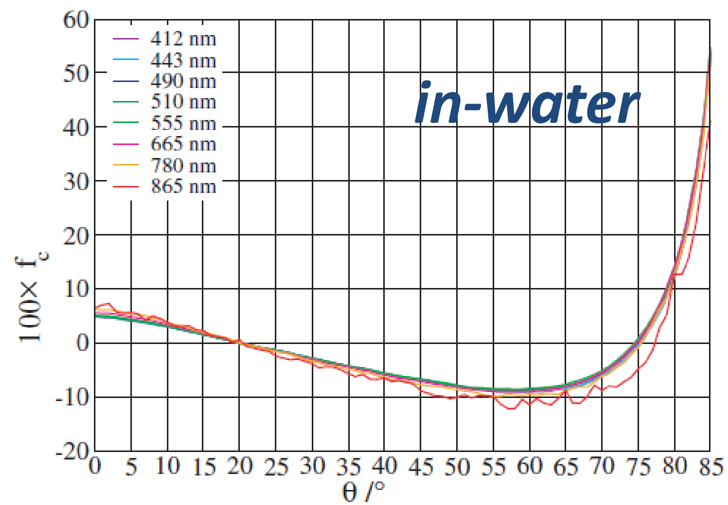

Cosine error

$$f_c(\phi, \theta, \lambda) = \left[\frac{E_N(\phi, \theta, \lambda)}{cos(\theta)} - 1\right]$$

Cosine error for a number of RAMSES irradiance sensors

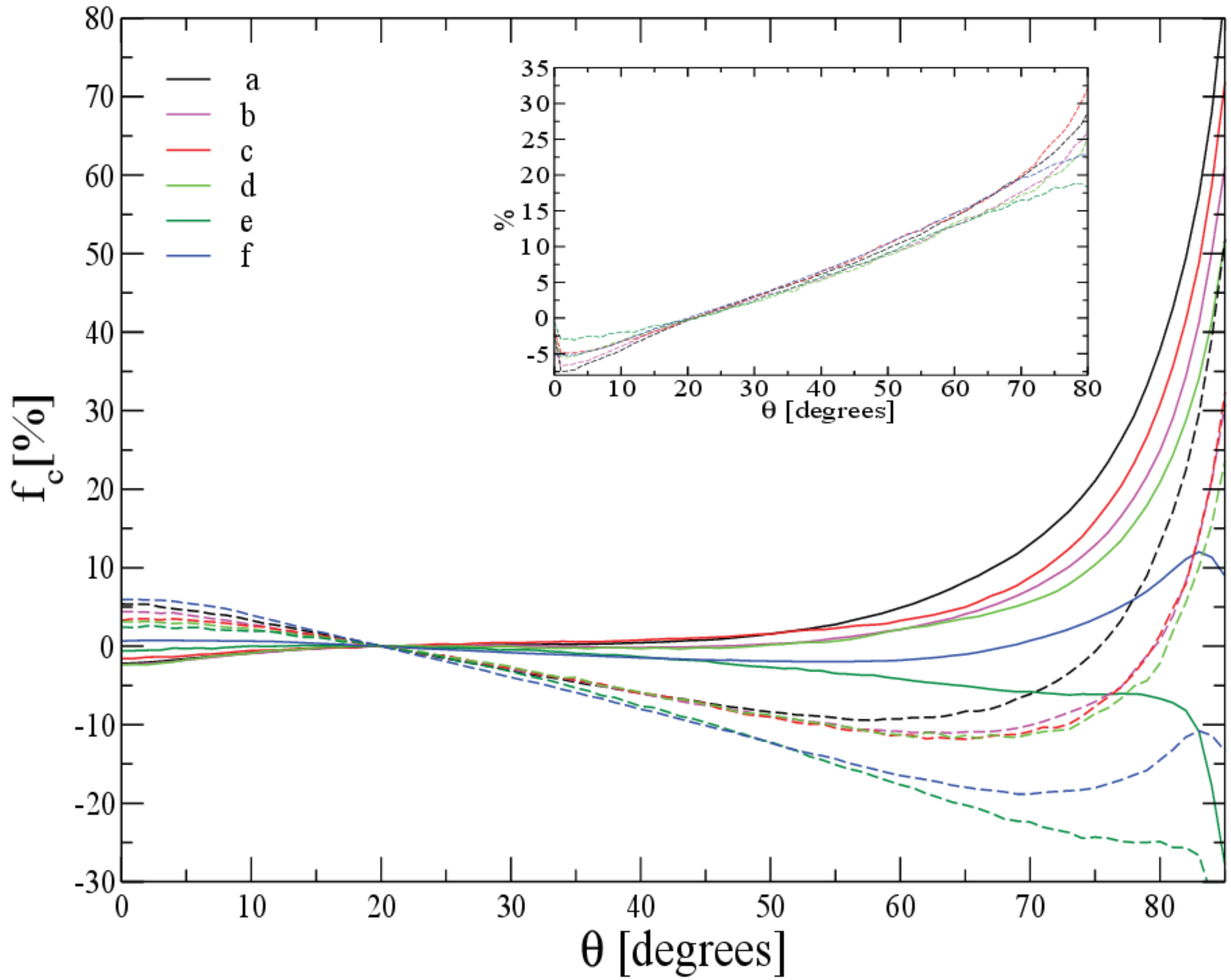

S. Mekaoui and G. Zibordi. Cosine error for a class of hyperspectral irradiance sensors, Metrologia 50 (2013).

Temperature response

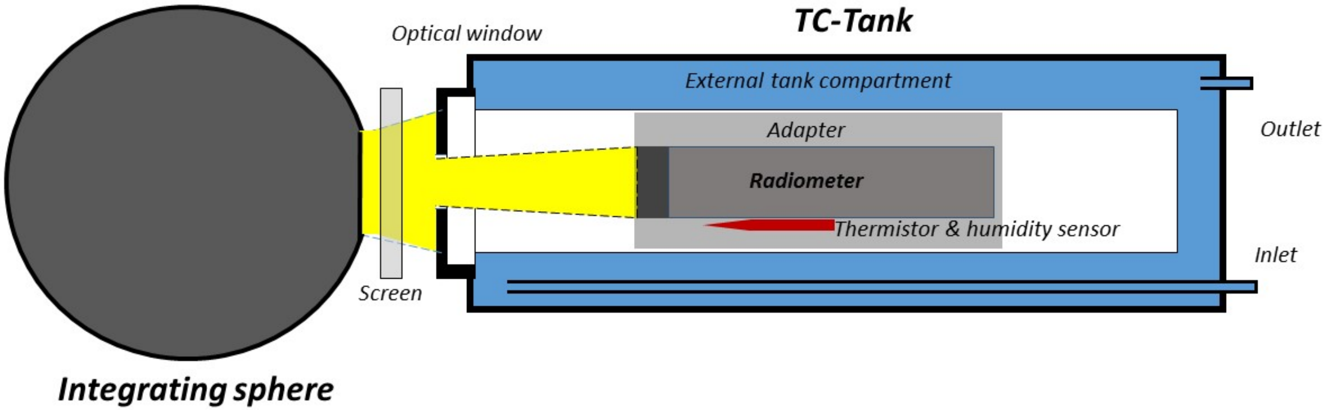

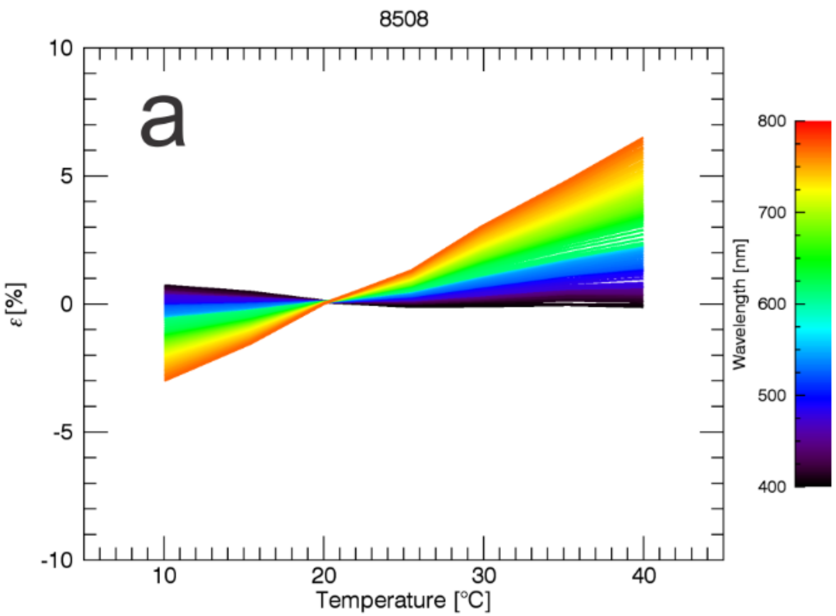

Change in response with temperature

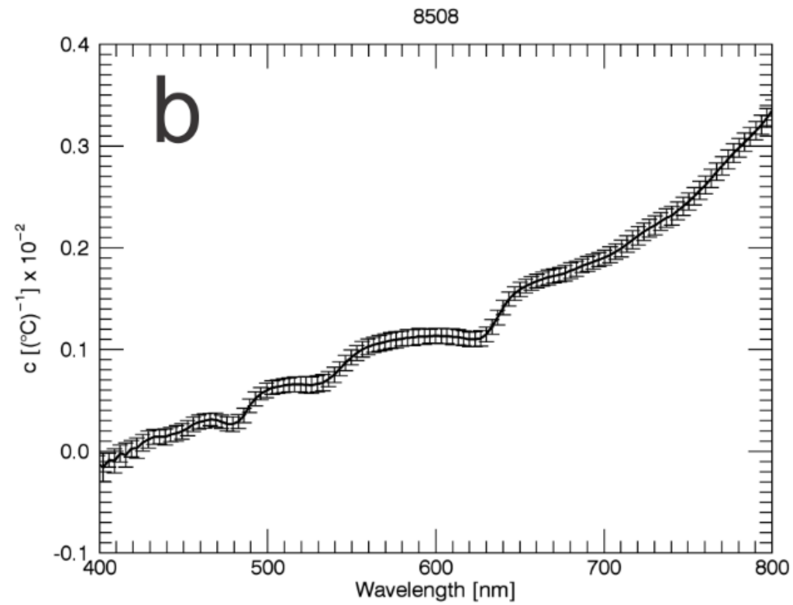

Temperature coefficient

Zibordi, G., et al., 2017. Response to Temperature of a Class of In Situ Hyperspectral Radiometers. Journal of Atmospheric and Oceanic Technology, 34(8), pp.1795-1805.

Joint Research Centre

Temperature response: results

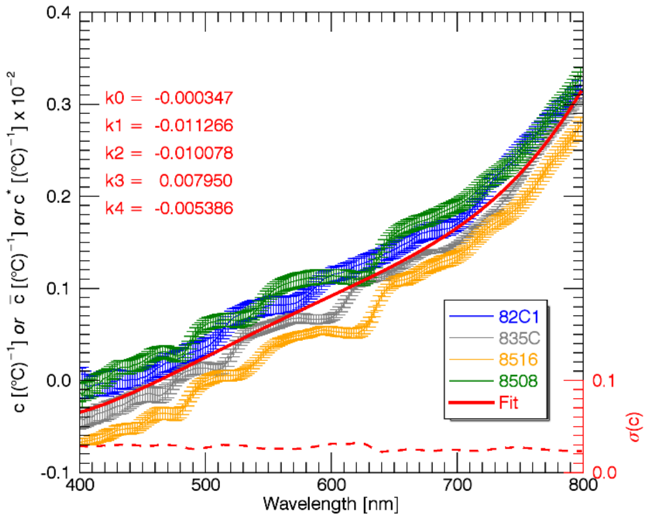

Change in response (RAMSES)

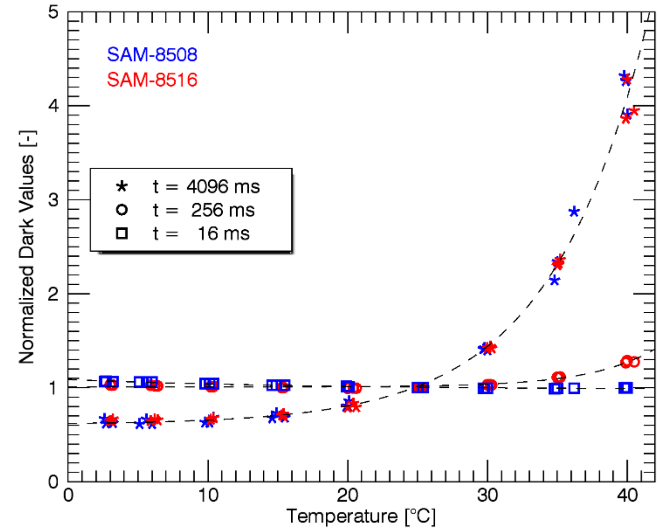

Dark signal (RAMSES)

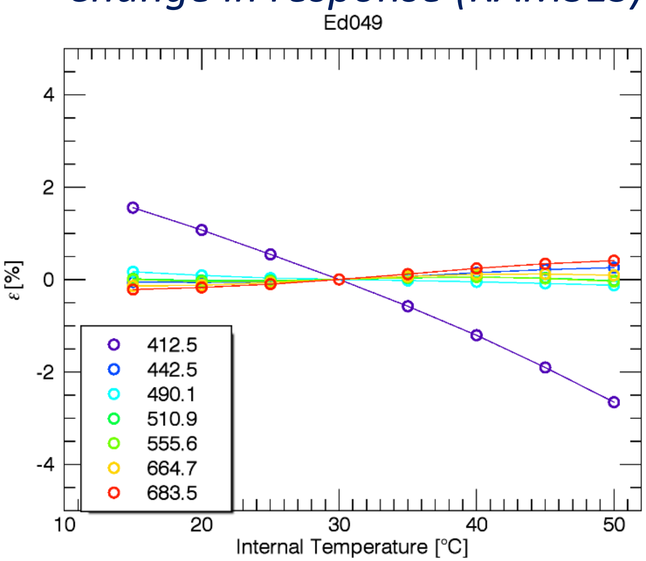

Change in response (OCR 507)

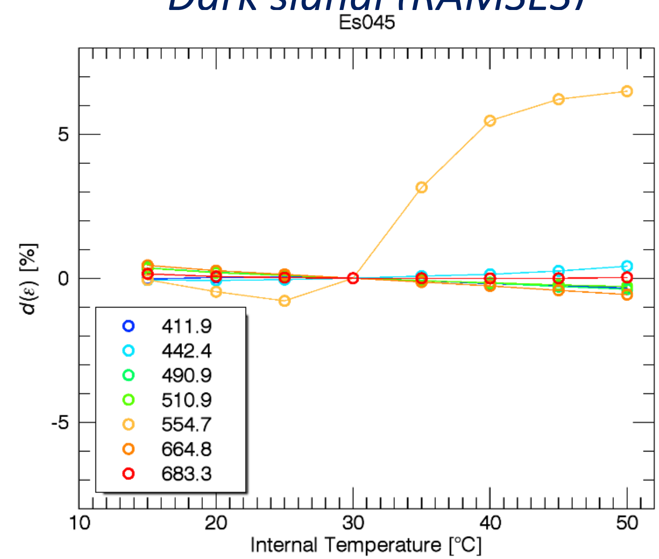

Degradation (OCR 507)

Zibordi, G., et al., 2017. Response to Temperature of a Class of In Situ Hyperspectral Radiometers. Journal of Atmospheric and Oceanic Technology, 34(8), pp.1795-1805.

Polarization sensitivity

(a)

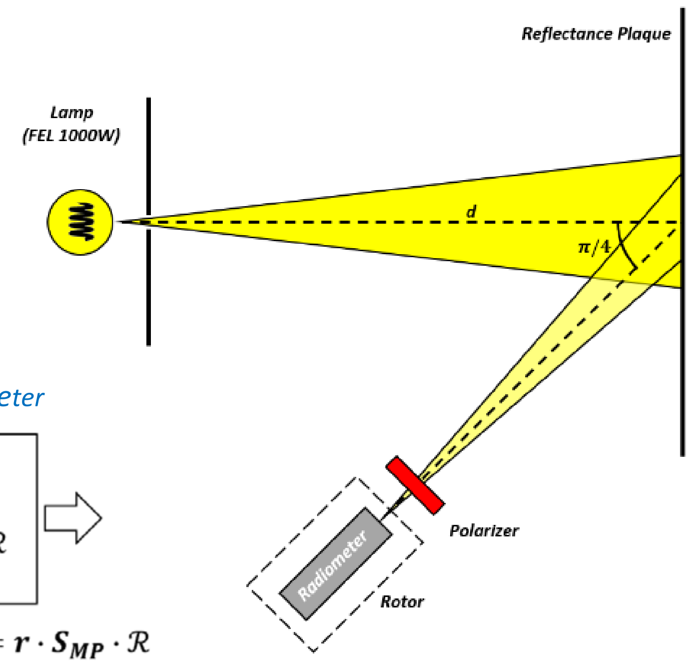

Measurement configurations applied for the determination the polarimetric characteristics of radiance sensors

Flow diagram for the determination of the polarimetric characteristics of a radiometer

SOURCE → POLARIZER $P(s,d,p,q)$ → ROTOR $M(\phi)$ → RADIOMETER $r(R_{00},r_1,r_2,r_3),\mathcal{R}$ →

$\boldsymbol{S}$ $\quad$ $\boldsymbol{S_P} = \boldsymbol{P}\cdot\boldsymbol{S}$ $\quad$ $\boldsymbol{S_{MP}} = \boldsymbol{M}\cdot\boldsymbol{S_P}$ $\quad$ $\boldsymbol{DN} = \boldsymbol{r}\cdot\boldsymbol{S_{MP}}\cdot\mathcal{R}$

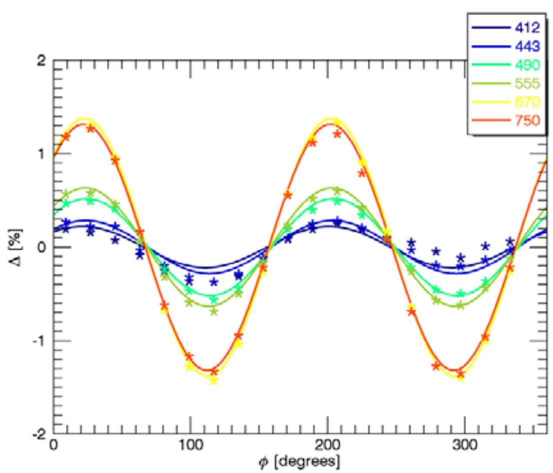

Difference in polarization sensitivity across rotation planes of RAMSES hyperspectral radiometers

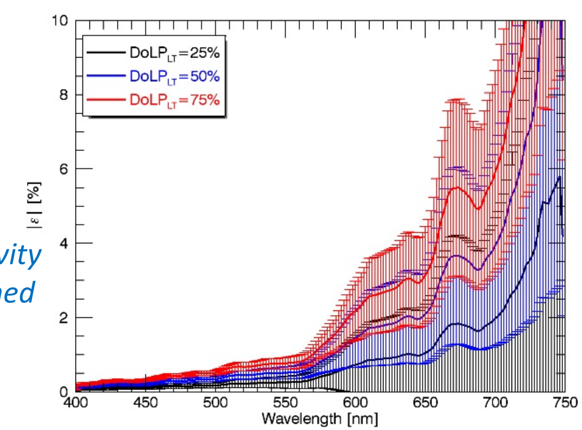

Impact of polarization sensitivity in Rrs measurements performed with RAMSES hyperspectral radiometers

Talone, M. and Zibordi, G., 2016. Polarimetric characteristics of a class of hyperspectral radiometers. Applied Optics, 55(35), pp.10092-10104.

Straylight effects

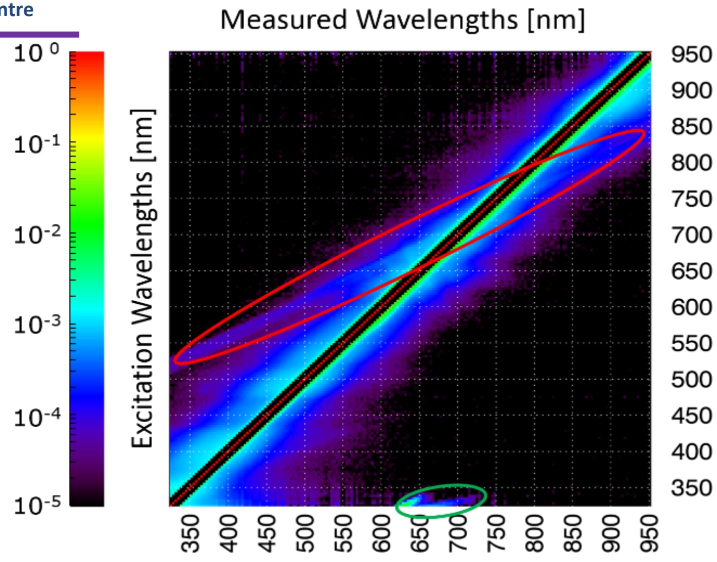

Stray light distribution matrix

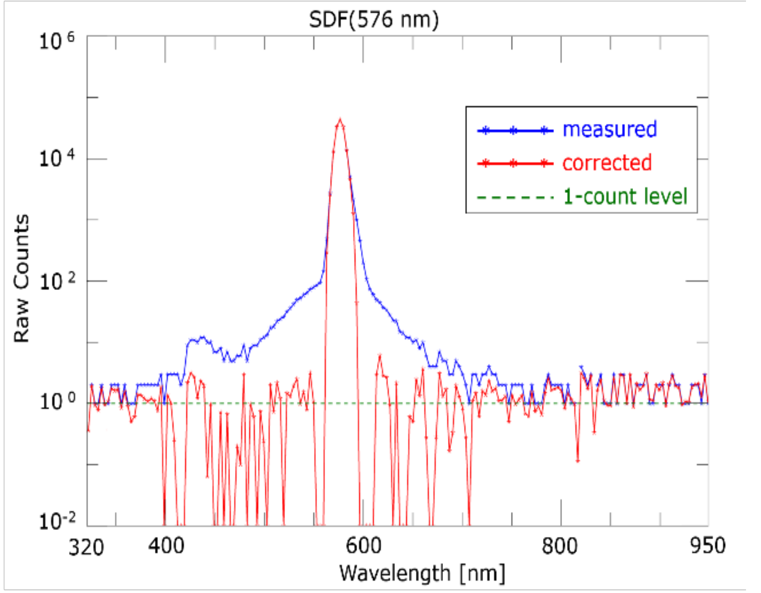

Line spread function

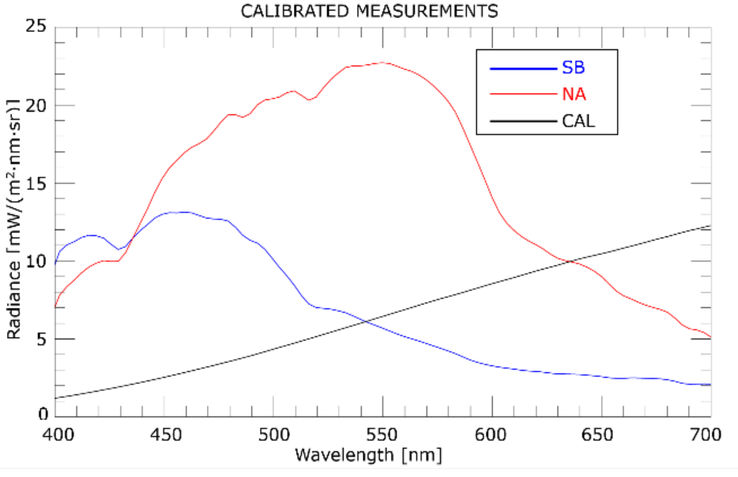

L_T for different waters

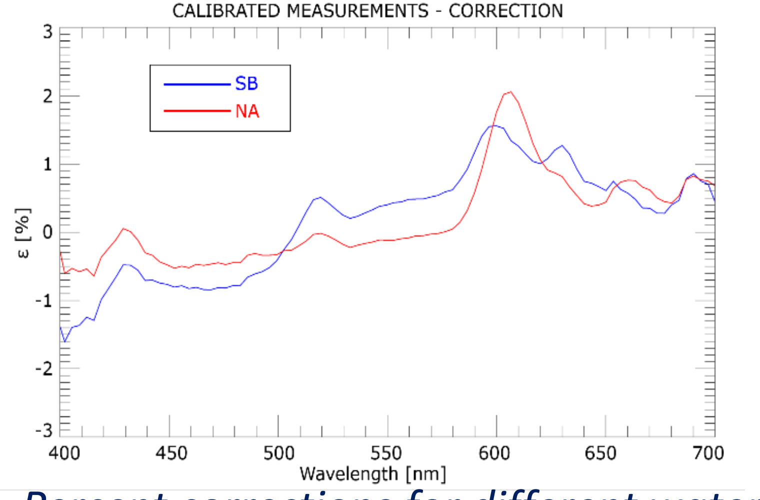

Percent corrections for different waters

Talone, M., Zibordi, G., Ansko, I., Banks, A.C. and Kuusk, J., 2016. Stray light effects in above-water remote-sensing reflectance from hyperspectral radiometers. Applied optics, 55(15), pp.3966-3977.

Joint Research

Nonlinearity

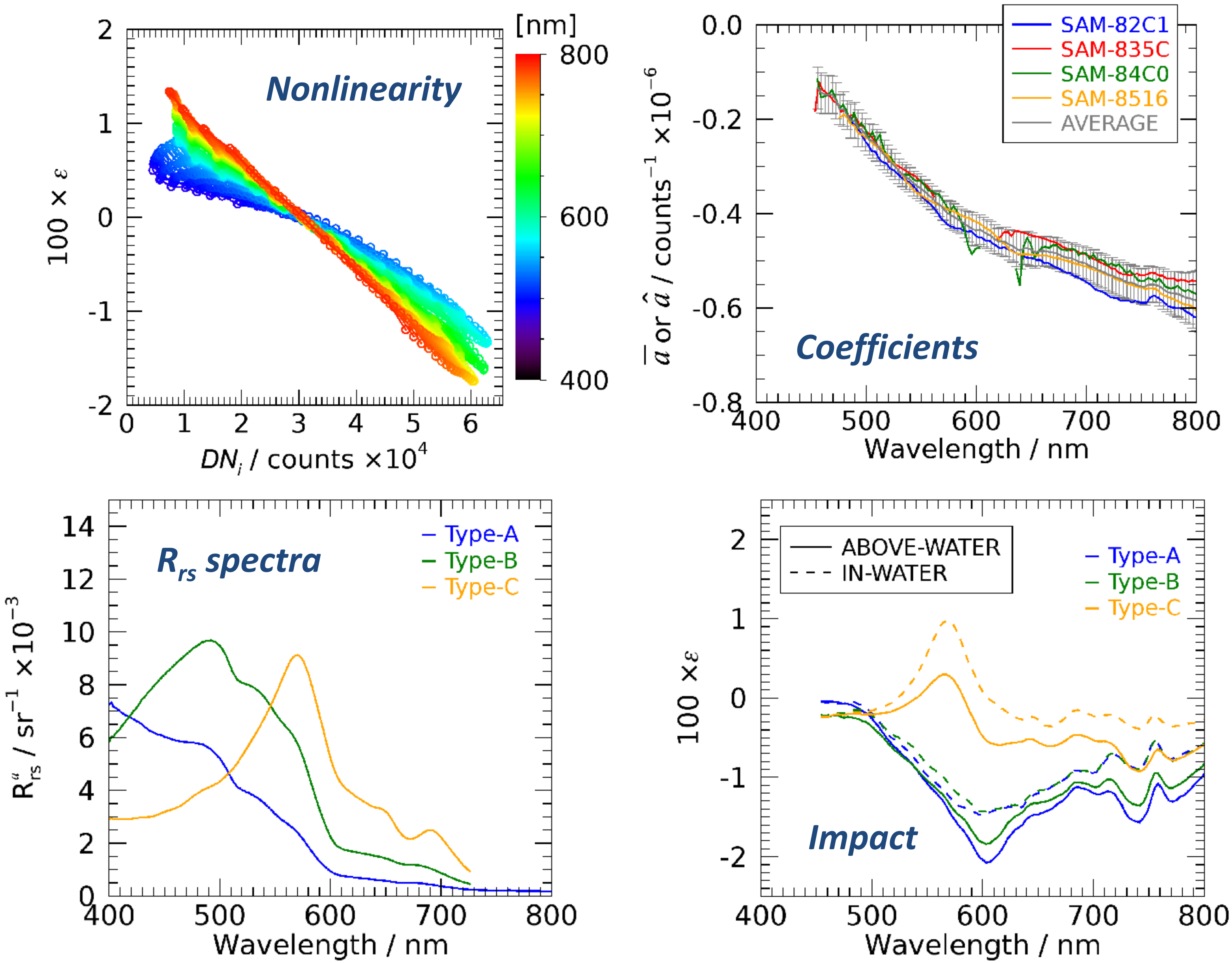

Talone, M. and Zibordi, G., 2018. Nonlinear response of a class of hyper-spectral radiometers*. Metrologia.*

Joint Research Centre

Example of uncertainty budget

Uncertainty budget (in percent) for L_W determined from in-water profile data (hyperspectral radiometer)

Uncertainty source	443		555		665	
Absolute calibration of L_u	2.7	2.7	2.7	2.7	2.7	2.7
Immersion factor	0.2	-0.6	0.2	-0.9	0.2	-1.2
Temperature response (+5C)		+0.2		-0.3		-0.7
Polarization sensitivity		+0.1		+0.2		+0.4
Stray-light effects		-1.0		+0.5		+0.5
Nonlinearity		-0.0		-1.0		-0.2
Self-shading correction	0.3	-1.2		-0.8	0.8	-3.2
Environmental effects	2.1	2.1	2.2	2.2	3.2	3.2
Statistical sum	**3.4**	**4.2**	**3.5**	**4.2**	**4.3**	**6.1**

$$\Im(\lambda) = C_{\Im}(\lambda)\ I_f(\lambda)\ \aleph(\lambda)\ DN(\Im(\lambda))$$

The above table includes contributions related to temperature response, polarization sensitivity, stray-lights, nonlinearity, i.e., $\aleph(\lambda) \neq 1$ (the radiometer does not have ideal performance).

Neglecting corrections may lead to an obvious underestimate of uncertainties. Noteworthy, compensation processes may minimize systematic effects for given measurement conditions with potential spectral impacts.

Joint Research Centre

Conclusions

A detailed characterization of field radiometers is the only way to ensure a comprehensive quantification of uncertainties. In fact, uncorrected systematic effects resulting from instrument miss-performance may differently affect uncertainties during diverse measurement conditions.

Full instrument characterizations are definitively essential for those instruments supporting key radiometric applications (e.g., system vicarious calibration or validation activities for climate applications).

Thanks